A Study of Printed Spiral Coils for Neuroprosthetic Transcranial Telemetry Applications

Maulik R. Shah, Richard P. Phillips, and Richard A. Normann,* *Member, IEEE*

Abstract— **We have explored the use of printed spiral coils (PSC's) for neuroprosthetic transcranial telemetry applications. We fabricated two-dimensional PSC's on a thin (25 μm) polyimide substrate using copper (35 μm) as a conducting material. All the coils had a fixed inner diameter of 1.0 cm. We fabricated two sets of coils. One set of coils consisted of 2- to 5-turn circular and square spiral coils and had different trace widths (W), different spacings (S) between adjacent traces, and different outer diameters. The other set of coils consisted of 5-turn circular spiral coils and had fixed inner and outer diameters but different W to S ratios. We measured loss resistances (R_s and R_p) and quality factors (Q) of these coils at different resonating frequencies in the range of 5–40 MHz. Over this frequency range, we observed that for fixed inner and outer diameters, the coil with the largest W achieved the lowest R_s and the highest R_p and Q. These electrical properties and the fact that these coils can conform to the complex convoluted cortical surface suggest that a PSC [15] can provide a viable alternative to a conventional wire-wound coil for neuroprosthetic transcranial telemetry applications.**

Index Terms— **Coil efficiency, coil losses, neuroprosthesis, printed spiral coil, transcranial telemetry system.**

I. Introduction

RESEARCHERS have demonstrated that by electrically stimulating the visual cortex of blind volunteer, spots of light (termed phosphenes) could be evoked where a sighted individual would normally have his/her visual field [2], [7]. If patterns of electrically evoked phosphenes can be systematically organized to convey useful spatial information, then a functional visual prosthesis could become a reality. These considerations, coupled with recent advances in the fields of silicon micromachining and microelectronics, have caused researchers to reexamine the possibility of developing a cortically based visual prosthesis for the blind. It is likely that silicon-based electrode arrays will become an integral part of such a visual prosthesis for accessing neurons of the visual cortex [20]. We have developed such an electrode array, fabricated on a 4.2 mm $\times$ 4.2 mm monolithic silicon substrate and containing 100 microneedles that project out of the substrate [14]. An advanced, silicon-based demultiplexing scheme has also been designed to select each of the 100 individual electrodes and inject a safe level of current through them in order to elicit a pattern of phosphenes [15]. Further, in order to access the implanted electrodes and the associated electronics, and to provide the required level of current for the electrical stimulation of the visual cortex, a suitable interfacing link (the link that connects the external power supply and the external electronics to the implanted visual prosthesis) is required.

In the previous designs of prototype visual prostheses, two types of interfacing links were implemented [2], [7]. These interfacing links were a telemetry system implemented by Brindley and his research group [2], and a multiple-lead wire-percutaneous connector system implemented by Dobelle *et al.* [7]. There are distinct advantages associated with the lead wire-percutaneous connector system: 100% efficient power transfer (providing for a long life of external batteries), wide bandwidth for data transfer, and no need for electronic circuitry to be attached with the implanted electrodes. However, the lead wire-percutaneous connector that breaches the skin and the skull, increases the chances of infection. As the lead wires are fastened to both the connector and the array, there is an increased chance of lead wire failure due to motion of the brain with respect to the cranium. This relative motion can cause forces on the array due to its being tethered to the connector, which increases the chance of lead wire failure and/or displacement of the implanted array. Further, patients are unlikely to accept a skull mounted connector for a chronic application. Considering these issues for a cortical neuroprosthesis (such as a visual prosthesis), a transcranial telemetry system across a closed scalp may offer advantages over a lead wire-percutaneous system. By eliminating a direct connection between internal and external components of the neuroprosthesis, the telemetry system substantially reduces the likelihood of infection and the consequences of tethering forces. However, the design of such a telemetry system offers more challenges than a lead wire-percutaneous connector system. Further, the use of implanted electronics mandates the use of hermetic sealing of the prosthesis to protect the circuitry from the corrosive environment of the cerebral spinal fluid. Considering these issues, we are beginning to implement a transcranial telemetry system to be used in the design of the visual prosthesis. The schematic diagram of the telemetry system, its associated components, and its integration with the electrode array and the demultiplexing chip are shown in Fig. 1 [19].

Designs of transcutaneous/transcranial telemetry systems for various neuroprosthetic applications have been reported in

Manuscript received January 4, 1995; revised January 14, 1998. *Asterisk indicates corresponding author*

M. R. Shah is with the Department of Bioengineering, The University of Utah, Salt Lake City, UT 84112 USA.

R. P. Phillips is with Link Research, Salt Lake City, UT 84111 USA.

*R. A. Normann is with the Department of Bioengineering, The University of Utah, Salt Lake City, UT 84112 USA (e-mail: normann@m.cc.utah.edu).

Publisher Item Identifier S 0018-9294(98)04381-X.

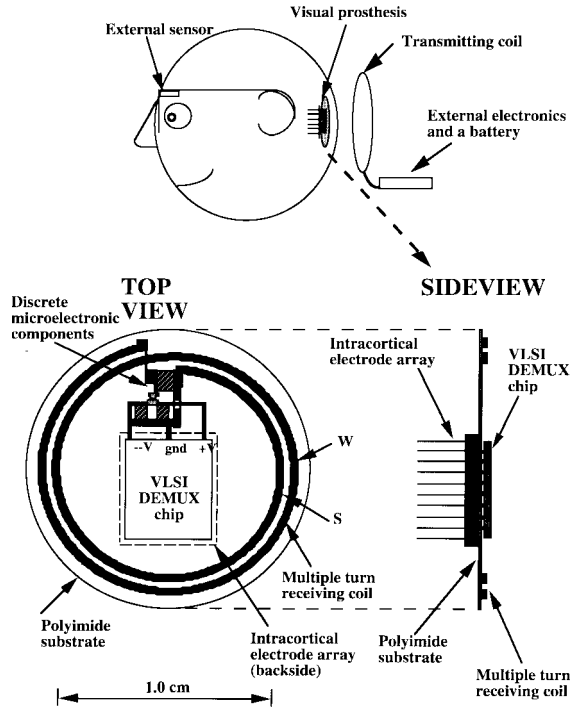

Fig. 1. Different components of the visual prosthesis and the telemetry system. An external transmitting coil will send power and data to the implantable receiving coil. The receiving coil will provide power and data to the demultiplexing chip and the electrodes. The component interconnection is made clear in the side view of the prosthesis, which shows the demultiplexing chip [built into a very large scale integration (VLSI) chip] connected to the electrode array in the plane of the receiving coil. The top view of the prosthesis shows the geometrical layout of the PSC and its interconnection with the electrode array and the demultiplexing chip.

the literature [2], [5], [8], [9], [13], [18], [21], [27]. Recent advances in silicon micromachining and silicon microelectronics [very large scale integration (VLSI) technology] have also enabled researchers to develop miniature neuroprosthetic devices that contain RF telemetry systems [16], [19], [26]. Despite the design variations in these telemetry systems, most use a multiple-turn, three-dimensional (3-D), wire-wound receiving coil as an internal component of the neuroprosthesis.

In a conventional wire-wound coil, different turns of the coil are stacked one upon another to achieve a multiple-turn coil with a "doughnut geometry." If such 3-D coils are to be used in a visual prosthesis application, they may not be able to conform to the convoluted surface of the cortex. The thickness of the wire-wound coil can be substantially reduced by orienting successive turns of the coil in a spiral geometry [two-dimensional (2-D)] rather than the doughnut configuration (3-D). Conformability of a wire-wound coil could be achieved by bonding a very thin wire in a spiral configuration to a thin and flexible substrate. These issues suggest that a thin, conformable, and biocompatible coil could be fabricated using simple photolithographic and microfabrication techniques. Further, as such a printed spiral coil (PSC) would be produced using standard photolithographic techniques, the geometric features of the coil can be precisely specified to address issues such as the skin and proximity effect on coil efficiency. The issue of skin effect (at high frequency) can be addressed by adjusting the thickness of the coil to be

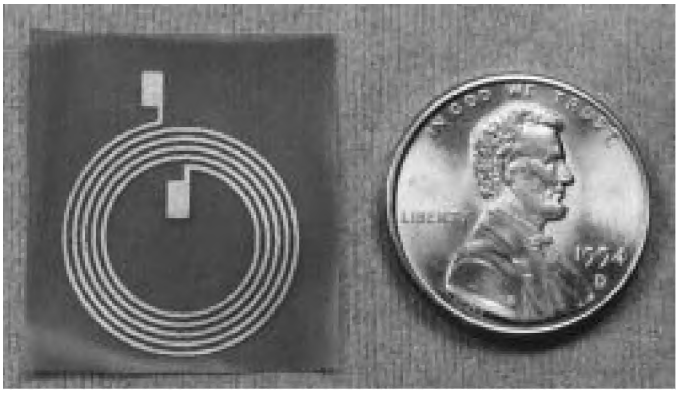

Fig. 2. A 5-turn circular spiral coil ($W = S = 313$ μm) fabricated on a flexible and biocompatible polyimide substrate.

appropriate to the skin depth at the frequency at which the coil is operated [4], [25]. The trace width (W) and the inner trace spacing (S) can be optimized to reduce the effect of proximity that could result due to the influence of current in the adjacent traces of the coil [4]. Further, the substrate upon which the coil is fabricated could provide an excellent insulating and encapsulating layer and could be used to mount discrete microelectronic components and provide interconnect traces for the electrode array and the demultiplexing chip. These aspects prompted us to fabricate and study the electrical properties of PSC's that could be useful in our neuroprosthetic transcranial telemetry application.

Researchers have described the electrical properties of cylindrical, closely packed wire-wound coils in the frequency range of 0.2–20 MHz, as well as the dependence of series (R_s) and parallel (R_p) loss resistances of such coils on resonating frequency and the number of turns in the coils [8]. Others have reported on electrical properties of printed thin film coils (fabricated on glass and ceramic substrates) designed to be operated in the frequency range of 100 MHz–1 GHz for nonbiological applications [4]. In this reported study, the optimum quality factor (Q) (for a coil with an outer diameter of 0.25 cm) was obtained when the W equaled to the S. Since no data were provided on the electrical properties of PSC's in the frequency range of 1–100 MHz, our study focused on the frequency range judged most appropriate for a transcranial telemetry application.

We fabricated PSC's on a thin, conformable, and biocompatible (polyimide) substrate using copper as a conducting material (Fig. 2). We fabricated two sets of coils. One set of coils consisted of 2- to 5-turn circular and square spiral coils and had a variety of W, S, and outer diameters. The other set of coils were 5-turn circular spiral coils with fixed inner and outer diameters and different W to S ratios (W to S ratios ranging from $W/S < 1$ to $W/S > 1$). We studied electrical properties of these PSC's in the frequency range of 5–40 MHz. Over this frequency range, we observed that for fixed inner and outer diameters, the coil with the largest W achieved the lowest R_s and the highest R_p and Q. These electrical properties and the fact that these coils are very thin and can conform to the complex convoluted cortical surface suggest that a PSC coil can provide a viable alternative to a

TABLE I
COIL DIMENSIONS OF DIFFERENT CIRCULAR AND SQUARE SPIRAL COILS WITH FIXED INNER AND VARIABLE OUTER DIAMETERS

Coils	Width	Spacing
Circular spiral coils	**W (μm)**	**S (μm)**
2, 3, 4 and 5 turn	163	250
2, 3, 4 and 5 turn	250	375
2, 3, 4 and 5 turn	250	313
2, 3, 4 and 5 turn	313	313
Square spiral coils	**W (μm)**	**S (μm)**
2, 3, 4 and 5 turn	125	375
2, 3, 4 and 5 turn	188	313
2, 3, 4 and 5 turn	250	250
2, 3, 4 and 5 turn	313	313

conventional wire-wound coil for neuroprosthetic transcranial telemetry applications.

II. MATERIALS AND METHODS

A. Coil Materials and Fabrication

Polyimide was chosen as the substrate of the PSC's described herein because of its demonstrated biocompatibility and because it has been widely used as an insulating material in a variety of neuroprosthetic applications [12], [17], [22]. Copper was selected as the model material because of its high conductivity and its commercial availability. However, since copper is not a biocompatible material, copper coils should be avoided in systems intended for chronic implantation. All our coils were fabricated from a commercially available cured polyimide (^{TM}Kapton)-based copper foil (Rogers Corporation, Chandler, AZ) using photolithographic techniques. The overall thickness of the PSC was approximately 90 μm, the thickness of copper was 35 μm, and the thickness of polyimide was 25 μm. The remaining thickness was due to the adhesive between polyimide and copper.

As the PSC was intended to be used along with the silicon-based Utah Intracortical Electrode Array [14], the inner diameter of all the PSC's was chosen to be 1.0 cm, a size large enough to contain the demultiplexing chip, the electrode array (on the back side), and a few discrete microelectronic components in the center of the coil (see Fig. 1). We fabricated two sets of coils. In one set of the coils, the outer diameter of the PSC was variable and was dependent on the number of turns and W and S of the coils. These coils were a set of 16 circular spiral PSC's and also a set of 16 square spiral PSC's with the number of turns varying from 2–5 having different W and S. We fabricated these coils in order to explore the electrical properties of PSC's and specifically to study the effect of coil geometry, operating frequency, number of turns, W, and S on the coil efficiency. Table I shows the dimensions of square and circular spiral coils.

The other set of coils were 5-turn circular spiral coils with fixed inner and outer diameters, but with a variety of W to S ratios (W/S). These coils were fabricated such that the center to center inner and outer diameters of all the coils were 1.0 and 1.625 cm, respectively. In between the outer and inner perimeters of the coil, a variety of 5-turn coils were fabricated such that the sum of W and S remained approximately constant. However, individual values of W and S varied from coil to coil providing different W to S ratios for the coils (see Table II). Further, depending on the width (W) associated with an individual coil (in this set of coils), the minimum and maximum inner and outer diameters varied approximately by 5% from the center to center inner and outer diameters of all the coils. We fabricated these coils in order to study the possible proximity effect due to different W to S ratio (W/S) as reflected in coil efficiency. Table II shows the values of W, S, and W to S ratios of these 5-turn circular spiral coils.

B. Analysis of Electrical Properties of Coils

In a telemetry system, the transmitting and receiving coils are inductively coupled to each other in order to transfer the required power and data from the transmitter to the receiver (see Fig. 1). In order to deliver the required level of power and data from the transmitter to the receiver efficiently, in most of the cases, the transmitting and the receiving coils operate at a particular frequency (most commonly the coil is operated at the resonant frequency determined by the coil and a parallel capacitor). The circuit in which the coil and a capacitor are connected to each other such that they resonate at a particular frequency is called a resonant circuit (also called a resonant tank circuit). There are two main configurations of the resonant circuits. One configuration is the series resonant circuit in which the coil is resonated by connecting a capacitor in series with it, and in another configuration, known as a parallel resonant circuit, the coil is resonated by connecting a capacitor in parallel with it. The losses associated with the resonant circuit are divided into coil losses and capacitive losses. However, using capacitors that have negligible losses, the resonant tank losses can be attributed to the coil losses.

The coil, acting as an inductor in either the series or parallel resonant tank circuit, has an intrinsic dc resistance associated

TABLE II
COIL DIMENSIONS FOR THE 5-TURN CIRCULAR SPIRAL COILS WITH FIXED INNER AND OUTER DIAMERERS AND DIFFERENT W TO S RATIOS

Coils	Width	Spacing	Width/Spacing
Circular spiral coils	**W (μm)**	**S (μm)**	**W/S**
5- turn coil	104	514	0.20
5- turn coil	152	462	0.33
5- turn coil	194	430	0.45
5- turn coil	228	391	0.58
5- turn coil	298	322	0.93
5- turn coil	351	265	1.32
5- turn coil	412	212	1.94

with it. This dc loss resistance of the coil mainly depends on the nature of the conducting material used in the fabrication of the coil, the length of the coil and the cross-sectional area of the coil. When the coil is operated at a high frequency, the losses associated with the coil are commonly represented by the series resistance of the coil (R_s), represented in series with the coil. However, in some cases, the losses associated with the coil, R_s, are represented by a parallel loss resistance, R_p. This ac resistance, R_s of the coil, depends on several factors such as the frequency at which the coil is being operated, the skin effect, the proximity effect, and eddy current effects due to metallic objects around the coil.

The quality factor (Q) of a coil is defined as how much energy it can store (in a coil inductor) versus how much energy it dissipates (by a series loss resistance, R_s). The relationship between the coil Q, coil inductance (L), and R_s is defined as

$$Q = (\omega^* L)/R_s. \tag{1}$$

The representation of Q in terms of R_s is one way to describe the quality of the coil. Another way is to represent coil losses is by a parallel loss resistance (R_p) that is represented as being in parallel with the coil. The relationship between the coil Q, coil inductance (L), and the parallel loss resistance (R_p) is defined as

$$Q = R_p/(\omega^* L). \tag{2}$$

Further, the relationship between R_s and R_p is defined as $R_p = R_s^*(Q^2 + 1)$ and can be further simplified as $R_p = R_s^*(Q^2)$ [or $Q = \sqrt{(R_p/R_s)}$], for $Q^2 \gg 1$. Thus, in order to characterize the coil Q one should know coil inductance, coil operating frequency, and either its series loss resistance (R_s) or its parallel loss resistance (R_p).

We estimated coil inductances using appropriate equations described in the literature [1], [4], [6], [11]. To validate the calculated values, coil inductances were measured using two different methods. The first method involved making a parallel tuned tank with a PSC and a capacitor of a known value and connecting that parallel tank in series with a resistor. A sinusoidal voltage was applied to the circuit from a variable frequency generator and the waveforms across the tank and tank plus the resistor were monitored with an oscilloscope. By bringing both the waveforms into phase, we could determine the resonant frequency of the tank. From the value of resonant frequency, the inductance of the PSC was then calculated. The second technique involved the use of an HP 4194A impedance/gain-phase analyzer. The calculated values of coil inductances differed from the measured values by no more than 10%–15% for all PSC's.

We measured the dc resistances of all PSC's with an LCR (inductance/capacitance/resistance) meter. Values of both the theoretically calculated and the measured dc resistances of PSC's were in close agreement. We also measured loss resistances R_s and R_p of all these coils at different resonating frequencies (the coils were resonated using different values of capacitance connected in parallel with the coil) in the frequency range of 5–40 MHz using the HP 4194A impedance/gain-phase analyzer. As the goal of the experiment was to achieve the greatest Q for a given coil, from the coils described herein, we characterized coils by calculating coil Q, using the relation between Q, R_s, and R_p: $Q = R_p/(\omega^* L) = (\omega^* L)/R_s = \sqrt{(Rp/Rs)}$, where ω is the resonating frequency, L is the coil inductance, R_s is the series loss resistance, and R_p is the parallel loss resistance.

III. RESULTS

The electrical properties of the PSC's were measured in an unloaded, parallel tuned tank model made from a parallel connection of the PSC and a capacitor. Since the capacitors were selected such that they had negligible losses, all tank circuit losses were attributed to coil losses and represented either by R_s or R_p. The parallel tank model was chosen so that direct comparison could be made between the R_p of the tank (R_p of the coil) and the load (computed from the power requirement of the electrode array) that will be placed in parallel with the parallel tuned tank. For an efficient telemetry system, most of the power that is received at the receiver tank should be delivered to the load, which can be achieved by making R_p of the parallel tuned receiver tank relatively high compared to the actual load (at resonance the receiver tank appears simply as a resistor). Thus, the goal of our study was to determine if a PSC could be fabricated that has a value of R_p substantially greater than the anticipated load resistance and that the PSC could provide the required value of Q.

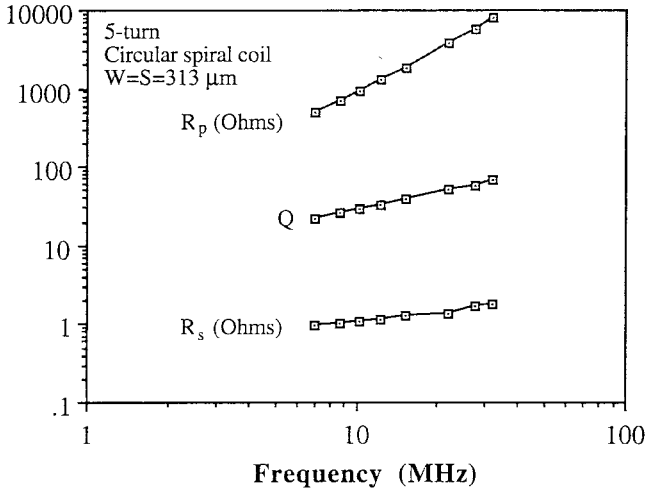

Fig. 3. The frequency dependence of series loss resistance (R_s), parallel loss resistance (R_p), and quality factor (Q) of a 5-turn circular spiral coil ($W = S = 313$ μm) at different resonating frequencies.

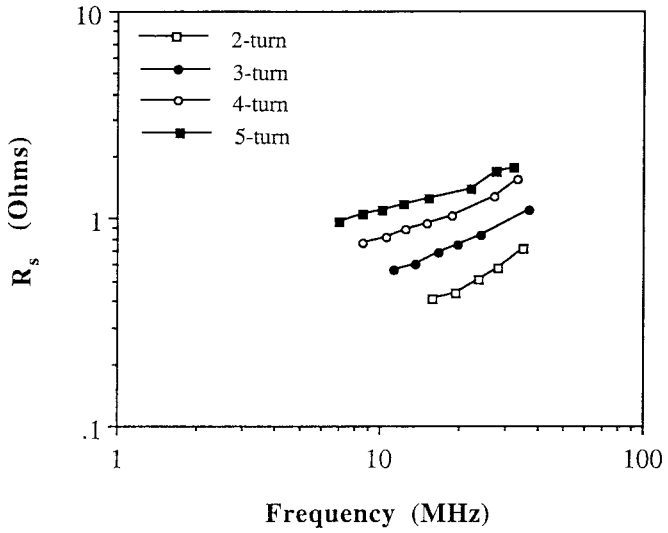

Fig. 4. Values of series loss resistance (R_s) of 2- to 5-turn circular spiral coils ($W = S = 313$ μm) at different resonating frequencies.

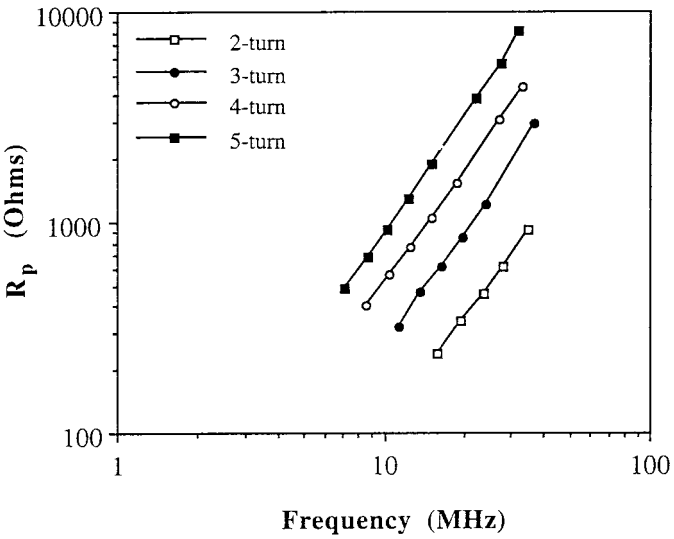

Fig. 5. Values of parallel loss resistance (R_p) of 2- to 5-turn circular spiral coils ($W = S = 313$ μm) at different resonating frequencies.

To investigate the frequency dependence of loss resistance of PSC's, we measured values of R_s, R_p, and Q for our sets of 16 circular spiral PSC's, 16 square spiral PSC's (with four different values of W and S and four different numbers of turns), and 5-turn circular spiral coils with fixed inner and outer diameters having different W to S ratios. These tests were conducted at various resonating frequencies (by creating a parallel tank using each PSC and resonating it at a particular frequency with an appropriate value of a capacitor), ranging from 5–40 MHz. The results, as shown in Fig. 3, show that R_s and Q have a square root dependence ($R_s \alpha \sqrt{f}$, $Q \alpha \sqrt{f}$) on the operating frequency. This has also been widely reported in the literature for other types of coils [4], [8], [25]. Since the relation between R_s and R_p can be approximated as $R_p = (\omega^* L)^2 / R_s$, if the frequency dependence of R_s is substituted in the relation, it is obvious that R_p has the frequency dependence of the order of $1.5(R_p \alpha f^{1.5})$. The dependence of frequency on the R_s, R_p, and Q of a 5-turn circular spiral coil ($W = S = 313$ μm) is shown in Fig. 3. A similar dependence was found for the coils with 2–4 turns.

The representation of the tuned tank losses (coil losses) by a parallel loss resistance (R_p) is one way to model the tank. A functionally identical model of tuned tank losses (the most common representation) is to represent the loss resistance of the coil as a series loss resistance R_s. A plot of values of R_s of PSC's with $W = S = 313$ μm and different number of turns (Fig. 4) illustrates the effect of resonating frequency and number of turns on the coil losses.

These results are similar to the results described in the literature for other types of coils [4], [8]. The coil losses increase with an increase in the number of turns and the operating resonant frequency. As it is convenient to replace R_s of the coil by R_p, similar PSC's were used to measure values of R_p at different resonating frequencies. Fig. 5 shows a comparison between the values of R_p of the PSC's (with $W = S = 313$ μm) having different numbers of turns, with the R_p increasing as either the number of turns or the resonating frequency (or both) increases. Although this effect is similar to the results shown for R_s (Fig. 4), the frequency dependence is greater for R_p than for R_s. This behavior has also been described by others for conventional wire-wound coils [8].

Since the frequency and number of turns of the coil have effects on coil losses that are similar to those seen in the conventional wire-wound coils, coil geometry is an important parameter in the design of the spiral configuration of the printed coils. Values of R_s for 5-turn circular PSC's with different W and S, measured at different resonating frequencies, are shown in Fig. 6. As the width of the coil increases, R_s of the coil decreases. The coil with the biggest W achieved the smallest R_s. This was also found to be true for any number of turns in the coil [2–4 in our case].

Values of R_p for 5-turn circular PSC's with different W and S, measured at different resonating frequencies, are also shown in Fig. 7. The PSC with $W = S = 313$ μm achieved the highest R_p at each resonating frequency (the PSC's have

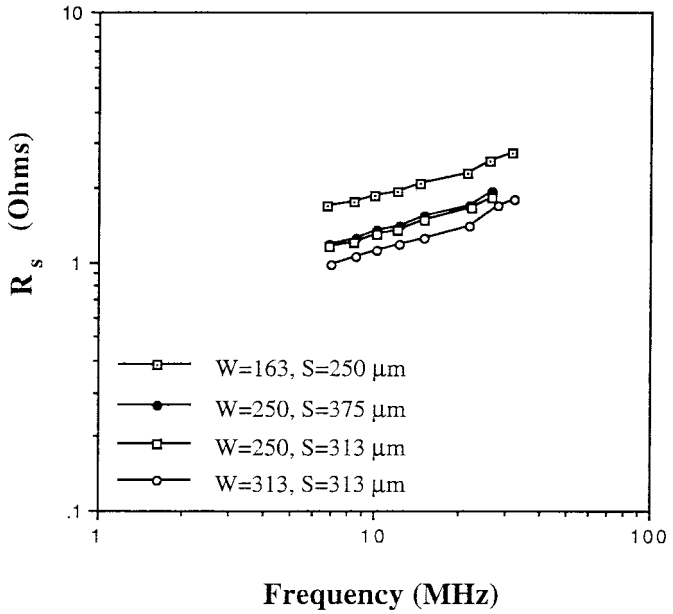

Fig. 6. Values of series loss resistance (R_s) of 5-turn circular spiral coils with different W and S at different resonating frequencies.

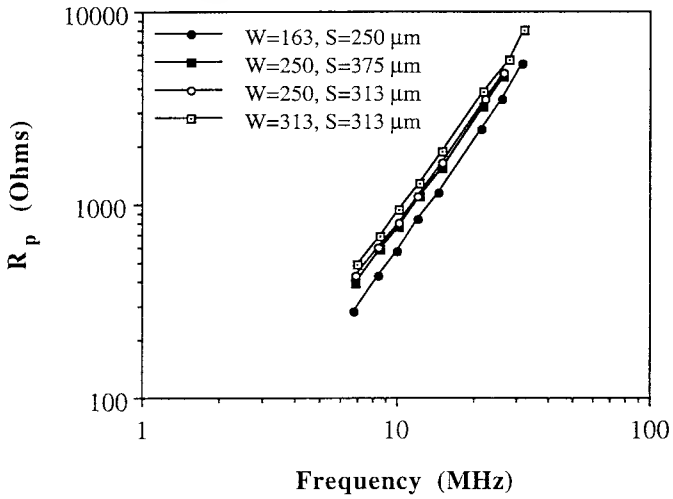

Fig. 7. Values of parallel loss resistance (R_p) of 5-turn circular spiral coils with different W and S at different resonating frequencies.

different outer diameters due to different W and S). This was also found true for all other coils with different numbers of turns (2–4). This is because R_s is inversely proportional to W. The coil with a larger W has a smaller R_s (see Fig. 6). As R_p is related to R_s by the relation, $R_p = [(\omega^* L)^2]/R_s$, a coil with a larger W (smaller R_s) has a higher R_p. The coil with $W = 250$ μm, $S = 313$ μm had only a small change in R_p compared to the coil with $W = 250$ μm, $S = 375$ μm. As W was the same in these two coils, the small change in R_p was due to the change in inductance resulting from the different S and the different outer diameter.

Since losses in the PSC's are reflected in coil Q, the results shown in Fig. 7 can be represented in terms of Q. These results are shown in Fig. 8, which show values of Q for 5-turn circular PSC's with different W and S. A PSC with $W = S = 313$ μm achieved the highest Q at all resonating frequencies. This was because the R_s associated with the coil with $W = S =$

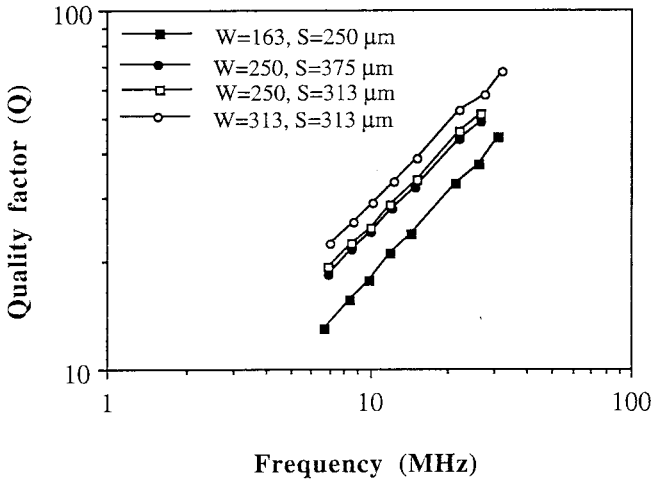

Fig. 8. Values of quality factor (Q) of 5-turn circular spiral coils with different W and S at different resonating frequencies.

313 μm was minimum. Further, as shown in Fig. 8, a change in width of the coil from 163 to 313 μm, resulted the change in Q by approximately 50% at 20 MHz. Further, the coils that had identical W, the coil with $W = 250$ μm and $S = 375$ μm and the coil with $W = 250$ μm and $S = 313$ μm, had a small change in Q caused by a change in S of the coil.

The above described coils (Figs. 3–8) had a fixed inner diameter and variable outer diameters. In these coils, the outer diameter was dependent on W, S, and the number of turns in the coil. However, in the design of a cortical neuroprosthetic device where miniaturization is an important issue, there is a restricted space available for the receiving coil. This constrains the size of the receiving coil and thus defines the inner and outer diameters of the coil. In between these inner and outer diameters of the coil, a certain number of turns can be provided by three different approaches: by making W less than S, W equal to S, and W greater than S. In order to study the effect of various W to S ratios on coil Q, we fabricated a set of 5-turn circular spiral coils that had fixed inner and outer diameters of 1.0 and 1.625 cm, respectively. Further, by keeping the sum of W and S approximately constant, various W to S ratios were obtained. We studied the effect of various W to S ratios on R_s, R_p, and Q of these coils at different resonating frequencies in the range of 5–40 MHz. The results of these coils at 21 MHz are shown in Fig. 9.

The top part of Fig. 9 shows the values of R_s for these coils for different W to S ratios. As shown in Fig. 9, R_s decreases as the W to S ratio of the coil increases. This is due mainly to the larger W associated with the coil. This is similar to what has been shown in Figs. 6–8. The remaining parts of Fig. 9 show the results in terms of R_p and Q. As R_p and Q are related to R_s such that any decrement in R_s is reflected as an increment in both R_p and Q, the coils with $W/S > 1$ achieved greater R_p and Q than coils with $W/S < 1$. Finally, the coil that had the biggest W ($W/S = 1.94$), in the set of all these coils, represented the lowest R_s and the highest R_p and Q. Finally, at 21 MHz, the values of R_s, R_p, and Q of the circular spiral coil with W to S ratio of 1.94 were 0.985 Ω, 4.774 kΩ, and 69.6, respectively.

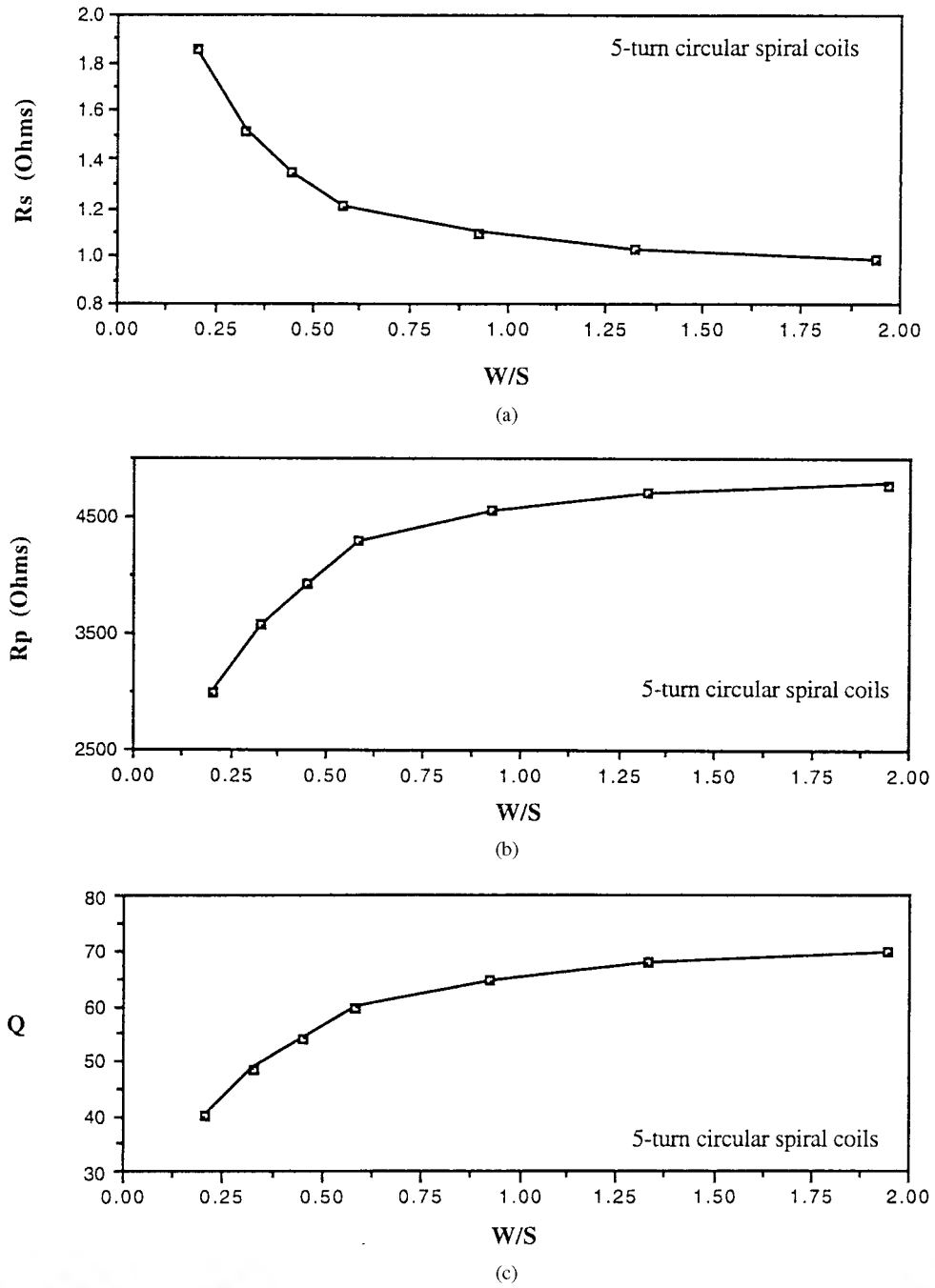

Fig. 9. Values of (a) R_s, (b) R_p, and (c) Q of 5-turn circular spiral coils with fixed inner and outer diameters and different W to S (W/S) ratios.

IV. Discussion

For the visual prosthesis under development at the University of Utah, we needed "surface mount space" in the center of the PSC for mounting the electrode array and the demultiplexing chip, as well as various discrete microelectronic components. Surrounding this required "surface mount space," we placed coils with 2–5 turns of either square or circular spirals. Because a circle has the minimum circumference for a given spacing between the inner edges of the coil, a square spiral geometry provides more area in the center of the coil and more inductance compared to a circular spiral coil of the similar dimensions. For similar numbers of turns, frequencies, and W and S dimensions, the dependence of coil losses (and Q) of square spiral PSC's were similar to those measured for the circular spiral PSC's. However, the consequences of misalignment between transmitting and receiving coils are greater for square spiral coils than for circular spiral coils (personal observations). Thus it would be preferable to use circular spiral coils rather than square spiral coils for a neuroprosthetic transcranial telemetry system.

A. Coil Electrical Properties

The PSC's that we have built achieved electrical properties similar to other coils that have been described in the literature. A previous study on the coil losses of resonant wire-wound

coils demonstrated that the R_s of circular wire-wound coils changes by a factor of 1.5 for every doubling of the resonating frequency [8]. However, this compares only the relative values of coil losses at different resonating frequencies. In order to compare the efficiencies of wire-wound coils and PSC's, we have normalized the series loss resistance (ac resistance) of both the types of coils (measured at 30 MHz for PSC's and extrapolated to 30 MHz for wire-wound coils) to their dc resistances. The ratio ($R_{\rm ac}$ to $R_{\rm dc}$) for PSC's was approximately four times smaller than their wire-wound counterparts described in the literature [8]. This suggests that our coils are less lossy than the wire-wound coils because the increase of coil resistance from its dc value to ac value (at a particular frequency) was smaller in our coils than the wire-wound coils.

The qualities of PSC's have been the subject of one other study in which the printed thin film coils were fabricated on ceramic and glass substrates [4]. This study focused on the electrical properties of printed thin film coils in the frequency range of 100 MHz to 1 GHz for nonbiological applications. The coils differed from our PSC's in terms of size, substrate material, substrate thickness, frequency of operation, and the model of the coil circuit (resonated tank in our case, self-resonated tank in their case). An empirical relationship was derived in the previous study that allows the determination of the series loss resistance, R_s, of any coil (with any dimension) at any frequency [4]. However, a constant that was used in the empirical relationship was derived to fit the data that were taken for their printed thin film coils in the frequency range of 100 MHz to 1 GHz. We calculated values of R_s for our PSC's based on this relationship in order to compare the results. The predicted frequency dependence of our PSC's agreed with the measured values. However, the absolute values of R_s for our PSC's agreed only roughly with this empirical relationship. We do not have any solid reasons to explain this, however we can only speculate that the constant that was calculated in order to fit the data taken for the printed thin film coils operated in the frequency range of 100 MHz to 1 GHz, did not fit well with the values of loss resistances of our PSC's. Further, for our PSC's in the frequency range of 5 to 40 MHz, we could not find the effect of proximity that was described for the printed thin film coils by others [8]. We could not find any optimum W/S ratio, instead we found a dominating W effect on the coil losses for the our PSC's: the greater is the width (W) of the coil, the greater is the coil Q (see Fig. 9).

B. Mutual Inductance Between Spiral Coils

Because we have developed a PSC with a 2-D geometry in order to reduce the height of the coil, we are forced to use a spiral configuration of the coil to achieve multiple numbers of turns. Since we are proposing the use of a PSC for telemetry applications, the mutual inductance between two circular spiral PSC's (transmitting and receiving coils) should be calculated. The calculation of the mutual inductance between two circular coils is described in the literature [18]. Similar analysis can be done between two circular spiral coils. However, because the radius of the spiral coil is varying, the calculation of mutual inductance between two spiral coils involves the solution of more complicated elliptic integrals compared to the solution of mutual inductance between two circular spiral coils and is beyond the scope of this paper. As an alternative to a complex theoretical calculation, the mutual inductance between multiple-turn spiral coils can be estimated by modeling the spiral coil as a summation of circular coils with different radii. If the radii of different circles are averaged, a multiple-turn spiral coil can be approximated as a multiple-turn circular coil. Finally, when the values of average radii of the spiral coils are substituted in the equations described in literature, the values of mutual inductance between two circular spiral coils can be estimated and would provide a close approximation of the value of the mutual inductance between two circular spiral coils.

C. Biocompatibility of PSC's

As the receiving coil will be implanted subdurally between the skull and the surface of the cortex, biocompatibility of the materials that are selected for the PSC must be favorable for chronic applications. Polyimide, selected as the substrate, has attractive insulating and biocompatible properties [12], [17], [22]. However, the copper used in our coils, although highly conductive, is not biocompatible. Therefore, potential biocompatible materials such as gold or platinum, must be used for making implantable coils. Gold is a possible alternative to copper and has conductivity closer to that of copper. Platinum is very biocompatible and has been widely used for the neuroprosthetic applications [7], [21]. There are two issues that need to be considered with platinum: 1) its bulk resistivity is six times higher than that of copper which might reduce the Q of coils by a factor of approximately two or three compared to copper coils of similar sizes; and 2) as the conductivity of the material decreases, its skin depth increases requiring the use of thicker platinum coils in order to achieve efficient operation at the desired frequency [3].

D. Encapsulation of the Visual Prosthesis

The PSC that has been designed, fabricated, and evaluated here is intended to be used in an implant system that will be chronically used in a human visual prosthetic system. The long-term application of the prosthetic device in an elevated temperature and high salt environment is a challenging task. We have taken a more robust approach for the chronic functionality of the prosthesis. We have selected and will be selecting biocompatible materials in the design of the electrode array, demultiplexing chip, and the receiving coil that will ultimately be used in the final design of the visual prosthesis. This approach guarantees the safety of the prosthesis in the situation where the encapsulation material starts failing. However, the safety of the prosthesis must be ensured by a suitable and biocompatible encapsulating material that can seal and protect the prosthesis against the body fluids and protect the body tissues from any harmful leaching of byproducts

from the prosthesis. Further, the successful application of a suitable encapsulant to the prosthesis also depends on the size and the shape of the prosthesis. In the design of the visual prosthesis we have ensured its miniaturization and we propose to select a suitable encapsulating material from a wide variety of materials such as silicone elastomers or gels, Parylene C, silicon nitride (or any other suitable material) that will ensure long-term functionality of the visual prosthesis.

We have focused much of our work on evaluating the coil efficiencies (quality factors) of these PSC's that can be used for our neuroprosthetic transcranial telemetry application. The goal of our study was to determine the parameters that would affect the value of R_p (or Q) of the PSC so that the value of R_p is substantially greater than the anticipated load resistance. We indicate that there are three major ways one can achieve the higher value of R_p (or Q) of a coil. One can operate a given size of the coil at a higher frequency (Figs. 3–8). If one is limited by the "safe" higher frequency, one can increase the number of turns and change the size of the coil (outer diameter) to achieve an acceptable high value of R_p (or Q) (Figs. 5–8). If the size and the operating frequency are constrained, one can improve the coil R_p (or Q) by varying the W to S ratios (Fig. 9). However, one has to keep in mind that the overall telemetry efficiency is not be sacrificed.

We had chosen to investigate the coil losses of PSC's in the frequency range of 5–40 MHz. This frequency window was selected, based on the following considerations. Operating the coils at frequencies less than 5 MHz results in considerable coil losses of these coils (small Q). Further, for neuroprosthetic applications, a relatively high data transmission through the coil may be required. We have limited our upper frequency range to 40 MHz because tissue power absorption may begin to become significant [13]. However, as the power level being transmitted is very small (a few milliwatts), this upper frequency window could be extended. More *in vivo* experiments will be needed to optimize the safest upper telemetry frequency.

We have implemented a 5-turn PSC ($W = S = 313$ μm) in the first generation of the telemetry system which we have built [23]. Because the polyimide substrate used in the coils we fabricated was relatively thick, we propose to use a thinner layer of polyimide to make the PSC more conformable to the cortical surface. Once we have a functional demultiplexing chip and an acceptable encapsulating material, chronic animal experiments will be conducted and the *in vivo* performance of the PSC and the overall telemetry system will be evaluated.

This study has shown that circular or square spiral coils, fabricated using conventional photolithographic techniques, can form a useful component in the design of transcranial telemetry systems. The thin polyimide substrate, coupled with the thin metallized coils, make an extremely flexible coil that should be able to conform to the convoluted cortical surface. Further, these coils have efficiencies that are comparable with their conventional wire-wound counterparts. Thus, these PSC's should provide a viable alternative to wire-wound coils for neuroprosthetic transcranial telemetry applications.

REFERENCES

[1] H. E. Brayn, "Printed inductors and capacitors," *Tele-Tech and Electron. Industries,* pp. 68–69 and 120–124, Dec. 1955.

[2] G. S. Brindley and W. S. Lewin, "The sensations produced by electrical stimulation of the visual cortex," *J. Physiol. (London),* vol. 196, pp. 479–493, 1968.

[3] G. H. Brown, C. N. Hoyler, and R. A. Bierwirth, *Theory and Applications of.Radio-Frequency Heating.* New York: Van Nostrand, 1947, ch. 10, pp. 102–114.

[4] R. B. Brown, "Experimental study of Q dependence of thin film inductor geometry," in *Proc. Int. Symp. Hybrid. Micro. (ISHM),* 1973, pp. 1–5.

[5] G. M. Clark, Y. C. Tong, J. F. Patrick, P. M. Seligman, P. A. Crosby, J. A. Kuzma, and D. K. Money, "A multi-channel hearing prosthesis for profound-to-total hearing loss," *J. Med. Eng., Technol.,* vol. 8, pp. 3–8, Jan. 1984.

[6] H. G. Dill, "Designing inductors for thin film applications," *Electron. Design,* pp. 52–57, Feb. 1964.

[7] W. H. Dobelle, and M. G. Mladejovsky, "Phosphenes produced by electrical stimulation of human occipital cortex and their application to the development of a prosthesis for the blind," *J. Physiol.,* vol. 243, pp. 553–576, 1974.

[8] N. de N. Donaldson and T. A. Perkins, "Analysis of resonant coupled coils in design of radio frequency transcutaneous links," *Med., Biol. Eng. Comput.,* vol. 21, pp. 612–626, Sept. 1983.

[9] D. C. Galbraith, S. Mani, and R. L. White, "A wide band efficient inductive transdermal power and data link with coupling insensitive gain," *IEEE Trans. Biomed. Eng.,* vol. BME-34, pp. 265–275, Apr. 1987.

[10] H. M. Greenhouse, "Design of planar rectangular microelectronic inductors," *IEEE Trans. Parts. Hybrids. Pack.,* vol. PHP-10, pp. 101–109, June 1974.

[11] F. W. Grover, *Inductance Calculations: Working Formulas and Tables.* New York: Dover, 1973.

[12] H. S. Haggerty and H. S. Lusted, "Histological reaction to polyimide films in cochlea," *Acta Otolaryngol. (Stockh),* vol. 107, pp. 13–22, 1989.

[13] E. S. Hochmair, "System optimization for improved accuracy in transcutaneous signal and power transmission," *IEEE Trans. Biomed. Eng.,* vol. BME-31, pp. 176–186, Feb. 1984.

[14] K. E. Jones, P. K. Campbell, and R. A. Normann, "A glass/silicon composite intracortical electrode array," *Ann. Biomed. Eng.,* vol. 20, pp. 423–437, 1992.

[15] K. E. Jones and R. A. Normann, "An advanced demultiplexing system for physiological stimulation," *IEEE Trans. Biomed. Eng.,* vol. 44, pp. 1210–1220, Dec. 1997.

[16] G. E. Loeb, C. J. Samin, J. H. Schulman, and P. R. Troyk, "Injectable microstimulator for functional electrical stimulation," *Med., Biol. Eng., Comput.,* vol. 29, pp. NS 13–NS 19, 1991.

[17] G. E. Loeb, A. E. Walker, S. Uematsu, and B. W. Konigsmark, "Histological reaction to various conductive and dielectric films chronically implanted in the subdural space," *J. Biomed. Mater. Res.,* vol. 11, pp. 195–210, 1977.

[18] S. Mani, D. C. Galbraith, and R. L. White, "Radio frequency coils in implantable devices: Misalignment analysis and design procedure," *IEEE Trans. Biomed. Eng.,* vol. BME-34, pp. 276–282, Apr. 1987.

[19] B. Ziaie, M. D. Nardin, A. R. . Coghlan, and K. Najafi, "A single-channel implantable microstimulator for functional neuromuscular stimulation," *IEEE Trans. Biomed. Eng.,* vol. 44, pp. 909–920, Oct. 1997.

[20] R. A. Normann, "Visual neurorprosthetics—Functional vision for the blind," *IEEE Eng. Medicine, Biol.,* pp. 77–83, Jan./Feb. 1995.

[21] C. R. Pfaltz, Ed., "The University of Melbourne Nucleus Multi-Electrode Cochlear Implant," *Adv. Oto-Rhino-Laryngol.,* vol. 38, pp. 63–81, 1987.

[22] S. Schmidt, K. W. Horch, and R. A. Normann, "Biocompatibility of silicon-based electrode arrays implanted in feline cortical tissue," *J. Biomed. Mater. Res.,* vol. 27, pp. 1393–1399, 1993.

[23] M. R. Shah, R. P. Phillips, and R. A. Normann, "A transcutaneous power and data link for neuroprosthetic applications," in *Proc. 15th Ann. Inter. Conf., IEEE-EMBS,* 1993, pp. 1357–1358.

[24] S. J. Tanghe and K. D. Wise, "A 16 channel CMOS neural stimulating array," *IEEE J. Solid-State Circuits,* vol. 27, pp. 1819–1825, 1991.

[25] F. E. Termann, *Radio Engineers Handbook.* New York: McGraw-Hill, 1950, ch. 2, pp. 26–128.

[26] P. R. Troyk and M. A. K. Schwan, "Closed loop Class E transcutaneous power and data link for microimplants," *IEEE Trans. Biomed. Eng.,* vol. 39, pp. 589–598, June 1992.

[27] C. M. Zierhofer and E. S. Hochmair, "High efficiency coupling-insensitive transcutaneous power and data transmission via an inductive link," *IEEE Trans. Biomed. Eng.,* vol. 37, pp. 716–722, July 1990.

Maulik R. Shah received the B.E. degree in instrumentation and control engineering from L. D. College of Engineering, Ahmedabad, India, in September 1991. He joined the Department of Bioengineering, University of Utah, Salt Lake City, in September 1991, working on the development of transcranial telemetry link for neuroprosthetic applications. Soon after he received the M.S. degree in bioengineering in June 1995.

He returned to his home town, Ahmedabad, where he is presently working with the medical division of Wipro BioMed, Wipro Ltd., India. His long-term plan is to develop cost-effective health care products for his country.

Richard P. Phillips received the B.S. degree in materials science from the Massachusetts Institute of Technology, Cambridge, in 1963. He studied bioengineering at the University of Utah before beginning work on transcutaneous energy transmission systems at the Biotechnisches Labor of Dr. H. Schima at the Technische Universität Wein, Austria, in 1988.

He worked on characterization of silicon epitaxial layers at IBM Corp. and Sprague Electric. After operating a BMW motorcycle dealership in Burlington, VT, he was employed by General Electric in Saudi Arabia and Turkey. He has continued work on energy transmission at Link Research, Salt Lake City, UT.

Richard A. Normann (M'88) received the B.S., M.S., and Ph.D. degrees in electrical engineering from the University of California, Berkeley.

He joined the staff of the National Institutes of Health (NIH) in 1974 and, in 1979, he joined the faculty of the Department of Bioengineering at the University of Utah, Salt Lake City. He is currently a Professor of Bioengineering and holds Research and Adjunct Professorships in Ophthalmology and Physiology in the School of Medicine at the University of Utah. His research interests are parallel information processing in the vertebrate visual system, and neuroprosthetics (the development of functional interfaces to the nervous system).